

MARS Simulation of Beam Loss and New Collimator Impact on the CDF and DØ Subdetectors

L.Y. Nicolas[†], N.V. Mokhov and A.I. Drozhdin

Fermi National Accelerator Laboratory

P.O. Box 500, Batavia, Illinois 60510

[†] *Also University of Glasgow*

April 1, 2003

Abstract

Beam-gas interactions in the Tevatron and their impact on the CDF and DØ forward detectors are briefly described. Results of detailed MARS simulations of background rates are presented and an effect of a possible new collimator in the Roman Pots region is analyzed.

1 Introduction

Interactions of the Tevatron beams with residual gas has a noticeable effect on the the CDF and DØ detector performance [1]. A new shadow collimator (mask) at the A48 section of the Tevatron is to be installed during the summer 2003 shutdown to mitigate this problem. The need for this collimator has been extensively discussed at the Beam Halo Task Force meetings led by Mike Albrow [2]. It has originally been designed [1, 3] to have a two-fold function: protection of the CDF silicon detectors in the event of an abort kicker prefire (AKP) and reduction of the machine-related background at CDF. Similarly, such a mask can reduce the background rates in the DØ subdetectors. Recently, it has been shown [4] that the beam halo generated background in CDF is not a primary concern because the radiation field in the detector is dominated by $p\bar{p}$ -events. Still, such a collimator is a last line of defense against beam-gas induced backgrounds, therefore we have included this second function into consideration.

In the CDF case, the collimator would physically be located roughly 60 m from the interaction point (IP) on the proton side, in the vicinity of the Roman Pots detectors. A crucial aspect for its installation is the impact of this mask on the pots lifetime and background. The MARS14 Monte Carlo code [5] is used for these studies, both for the CDF and DØ Roman Pots. In this note, a contribution of $p\bar{p}$ -interactions is not considered.

2 Simulation Model and Source Term

Substantial efforts have been put to build a detailed MARS calculational model. It includes the CDF detector with its experimental hall (Fig. 1), a simplified DØ region and ± 150 m of the Tevatron structures around BØ and DØ with quadrupoles, dipoles, separators, Roman Pots, tunnel and surrounding dirt. It is used for realistic simulations to investigate short- and long-range effects of beam loss on backgrounds and radiation levels in the CDF and DØ subdetectors. In addition, a separate 4-m long simplified model was built to study the new collimator influence on the CDF and DØ Roman Pots (Fig. 1 (right)).

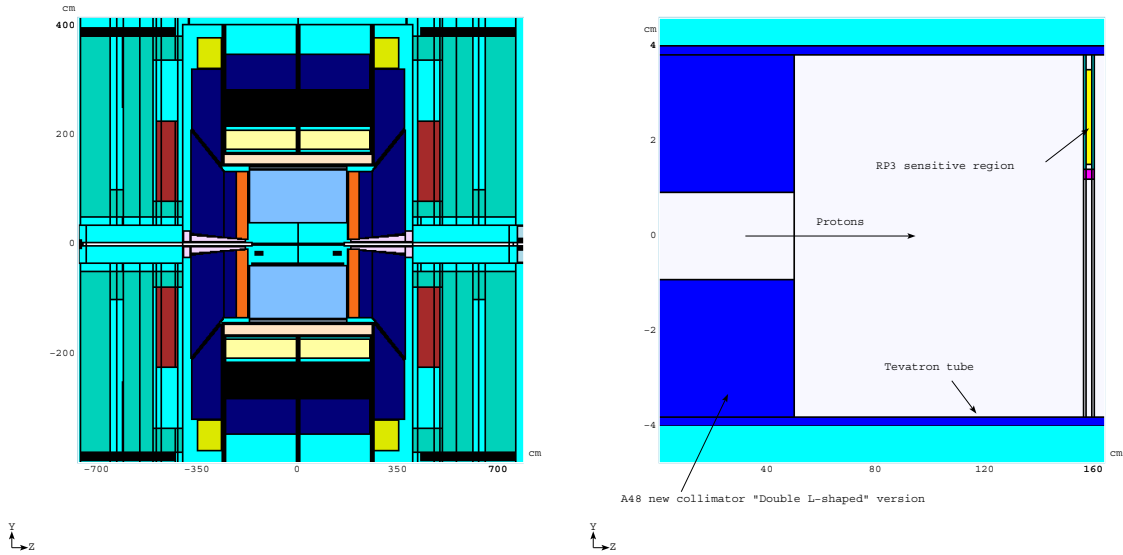


Figure 1: The CDF MARS model (left) and a mask/Roman Pot simplified model (right).

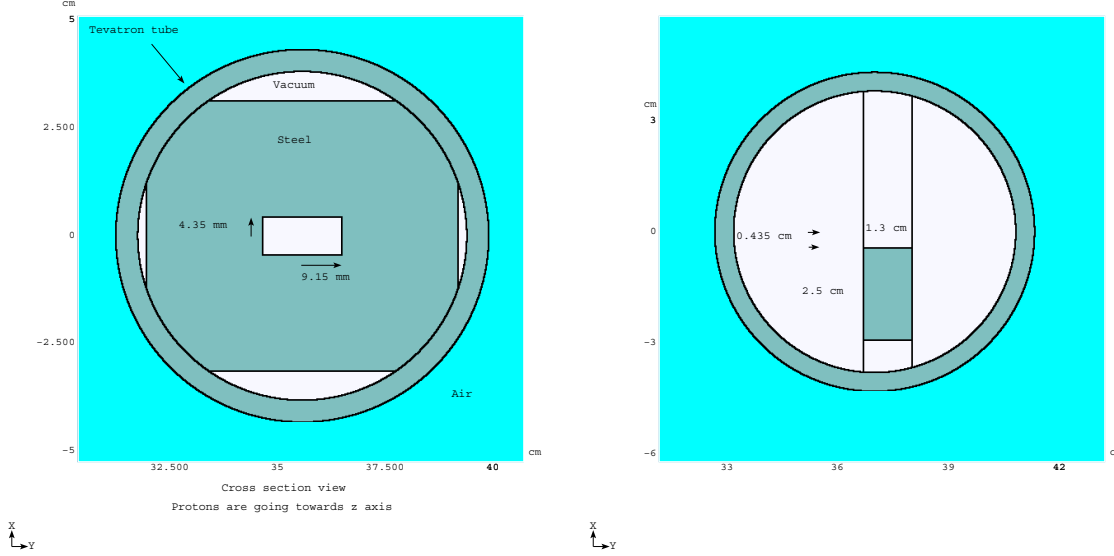


Figure 2: The A48 mask double L-shape (left) and minibar (right) versions.

The CDF dipole Roman pots (RP) set is composed of three detectors one meter apart from each other and starts with RP3 located at 58.6 m from the IP, for an incoming proton. The RP horizontal edge is at 12 mm from the beam pipe axis. The scintillator part of the RP facing the beam is $2 \times 2 \text{ cm}^2$. The DØ Roman Pots have the same sensitive area $2 \times 2 \text{ cm}^2$ but are based on the optical fiber technology.

Several shapes and lengths were investigated for optimization of the new collimator such as an aperture of $18.3 \text{ mm} \times 8.7 \text{ mm}$ for “double L-shape”, “single L-shape” and “minibar” A48 collimators (Fig. 2). For the “single L-shape” version, the bottom part of the “double L-shape” version remains as well as the vertical right part. The aim is the most effective protection of CDF in the event of an AKP with simultaneous minimalization of halo generated backgrounds in the RP.

A 1-TeV proton beam, 2×10^{11} ppb, 36 bunches at 47.77 kHz, were used in the calculations. Energy cut-offs in the MARS runs were 200 keV for all particles except neutrons with a threshold of 100 keV. Three components are used as a source term for the MARS studies:

- *Tails from collimators, i.e.*, beam loss in the 300-m region resulted from beam halo outscattered from the components of the *existing* collimation system [6]. At an average luminosity of $10^{32} \text{ cm}^{-2} \text{ s}^{-1}$, the proton beam leads to a rate of 3×10^7 p/s interacting with the primary collimators [6]. Phase space coordinates and a number of protons lost through this process are calculated with the STRUCT code [7].
- *Beam-gas elastic scattering, i.e.*, elastic nuclear scattering of a circulating beam on residual gas that leads to protons escaping the beam core, forming the beam halo and ultimately beam loss on the limiting apertures. This component of the source term in the same 300-m region is also calculated with STRUCT. In these multi-turn calculations, described in detail in Ref. [1], the average residual gas pressure in the ring is assumed to be 10^{-9} torr (or 10^{-10} torr as specified in the text).
- *Beam-gas inelastic interactions* are modeled directly in the course on the MARS runs. On contrary to the first two processes, particle production angles are relatively large here resulting in relatively short range tracing (tens of meters). A gas pressure in the vicinity of CDF and DØ is assumed to be 7×10^{-9} torr, leading to an interaction rate of $4334 \text{ m}^{-1} \text{ s}^{-1}$.

Fig. 3 shows contributions of the above three components to the background rates in the CDF West beam halo monitors (BHM) for two values of average gas pressure for elastic scattering for incoming protons. The BHM are about 50 cm around the beam pipe, at 18 m from the IP. Of course, partial accelerator-related background rates are different for different CDF and DØ subdetectors.

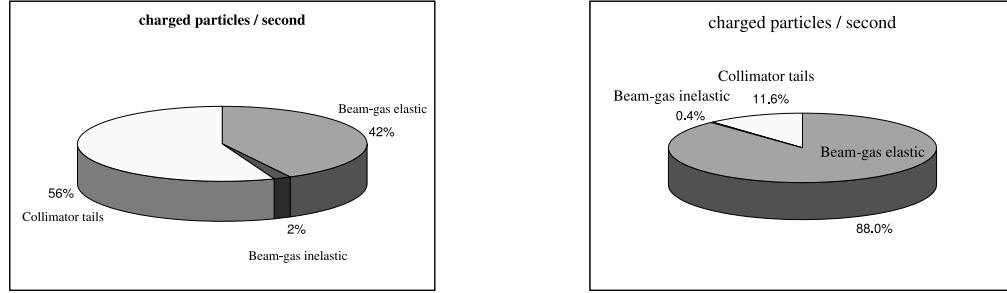


Figure 3: Contribution to BHM backgrounds at average pressure in Tevatron of 10^{-10} (left) and 10^{-9} (right) torr.

3 A48 Mask Effect and Comparison to Data

Fig. 4 (left) shows MARS-calculated charged particle flux in the CDF BHM with and without the “double L-shape” A48 collimator. The calculations were done with all three components of the beam loss source term, with an average pressure for elastic scattering of 10^{-10} torr. One sees that the collimator reduces the rates up to one order of magnitude (see also Fig. 12). The results without collimator are used to compare with recent measurements by Rick Tesarek [4]. Fig. 4 (right) compares his data with corresponding MARS results. A reasonable agreement is found. A some offset on the counter axis between measurements and simulation is to distinguish the points. This applies also to Fig. 5, Fig. 8 and Fig. 12. Fig. 5 (left) details two contributions (inelastic is negligible) at the BHM, while Fig. 5 (right) shows a distribution of protons hitting the “double L-shape” collimator for the beam-gas elastic component only. The impacts shown additionally for “minibar” and “single L-shape” versions demonstrate a poor efficiency to intercept protons.

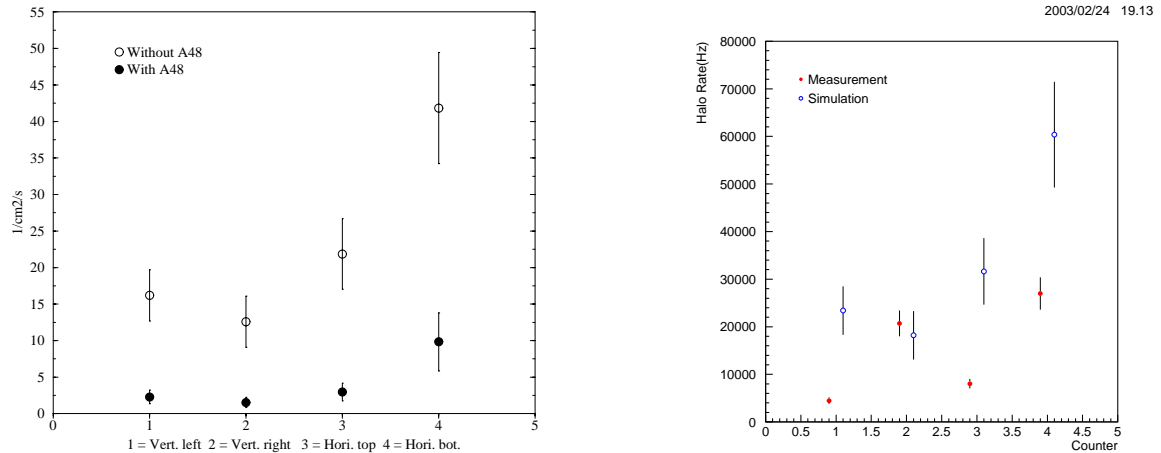


Figure 4: BHM hit rate with and without A48 collimator (left) and corresponding comparison of MARS calculations with data without the collimator (right).

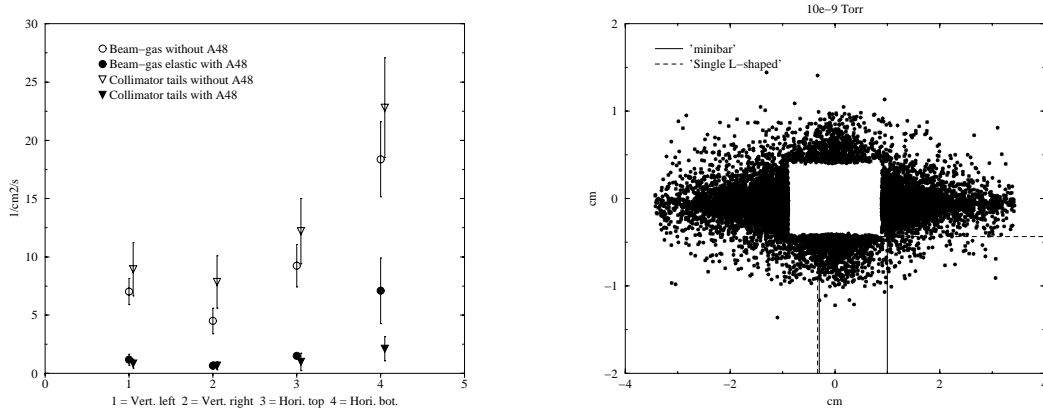


Figure 5: Comparison of two beam halo contributions at the BHM with and without the A48 mask (left) and spatial distribution of elastic beam-gas induced hits on the “double L-shape” collimator section (the entire plot), with lines showing the impact on “minibar” and “single L-shape” masks (right).

4 Roman Pots

Shadow collimators (masks) implemented in the vicinity of the CDF or DØ Roman Pots would certainly affect their performance.

4.1 Radiation damage

First question is the dose that the RP would receive due to low-energy particles generated in the collimator and if this would cause a premature degradation and affect the lifetime of the scintillator (silicon). Fig. 6 shows the rates in the RP with a “double L-shape” A48 collimator of different lengths due to beam halo interactions (left) and a single event of a kicker prefire AKP with a bunch of 2.78×10^{11} protons on A48 (right). The beam-gas elastic contribution is calculated for 10^{-9} torr on average. With a 0.5-m steel collimator (3 interaction lengths), 0.01 rad/s is an upper limit for the absorbed dose rate in the scintillator. With a 10^7 second physics year, it corresponds to 100 krad/yr. This is to be compared to 20 krad per a single AKP. Note, that good scintillators can withstand about 1 Mrad.

4.2 Background for diffractive physics

Another issue is the background that would disturb or possibly kill the diffractive physics studied with the RP. Only charged particle flux in the RP sensitive volume is of interest here. One of the concerns is the number of antiprotons coming from the IP and passing through the RP that would hit the collimator and then be backscattered towards the pots again. A simple MARS simulation has been performed with a 1-TeV beam on a 0.5-m long steel target. Two detectors were modeled, first 1 m upstream of the target, second 1 m downstream. The charged particle flux normalized to 1 proton is shown on Fig. 7 and include primaries and secondaries. The radius in the absciss represents the distance in respect to the initial beam axis. It appears that counts in the RP due to albedo would represent a tiny fraction of the background. At a 2.5 cm radius from the initial proton beam, for the worst case, the ratio albedo/forward is roughly 0.001.

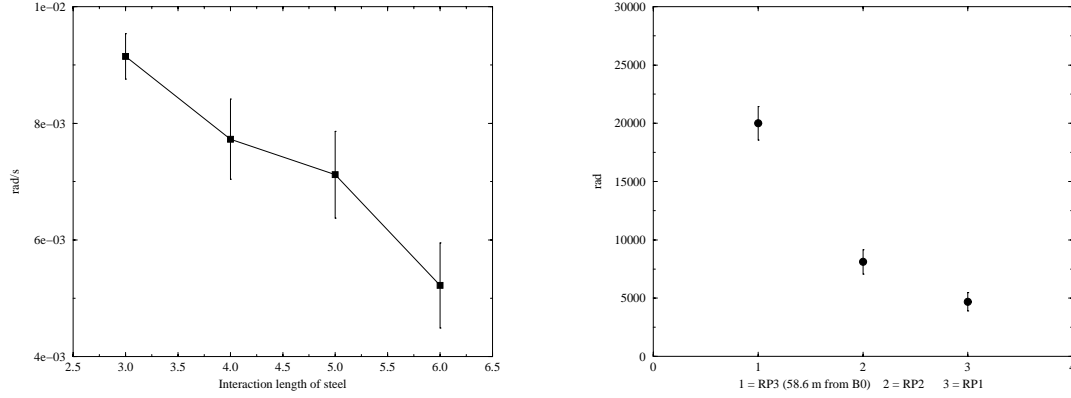


Figure 6: Absorbed dose rates in the RP3 due to beam halo (left) and dose in the RP1-RP3 due to AKP (right).

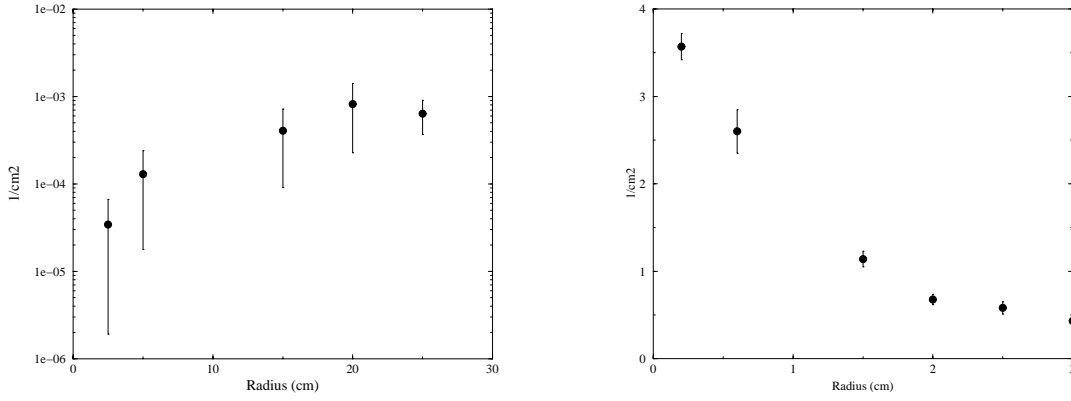


Figure 7: Charged particle albedo (left) and forward (right) flux in RP with a 0.5-m long steel rod.

4.3 Beam halo

Since the main purpose of the A48 collimator is a protection against AKP, in order to reduce the steel surface interacting with beam halo, simulations have been done to compare the charged particle flux reaching RP3 with the different shapes described earlier. The stainless steel collimator length was varied from 0.5 to 1 m, or 3 to 6 nuclear inelastic interaction lengths. This would leave at least 0.5 m of space between the end of A48 and RP3. Fig. 8 (left) shows the effect of the length and shape of the mask on the rate of charged particles in the RP3 calculated at 10^{-9} torr average pressure for beam-gas elastic scattering. Both secondary and primary particles contribute to the hit rate here. Results for “single L-shape” and “minibar” shapes are not discernable, but no major difference between the two was expected considering the distribution pattern for beam-gas elastic scattering shown in Fig. 5. One could thus keep the option of a “single L-shaped” collimator. The amplification factor due to the implementation of a “single L-shape” mask of six interaction lengths of steel reaches 4.5 compared to the rates without the collimator as predicted in [1]. For a 0.5-m long “double L-shape” collimator, this difference becomes an order of magnitude (Fig. 8 (right)).

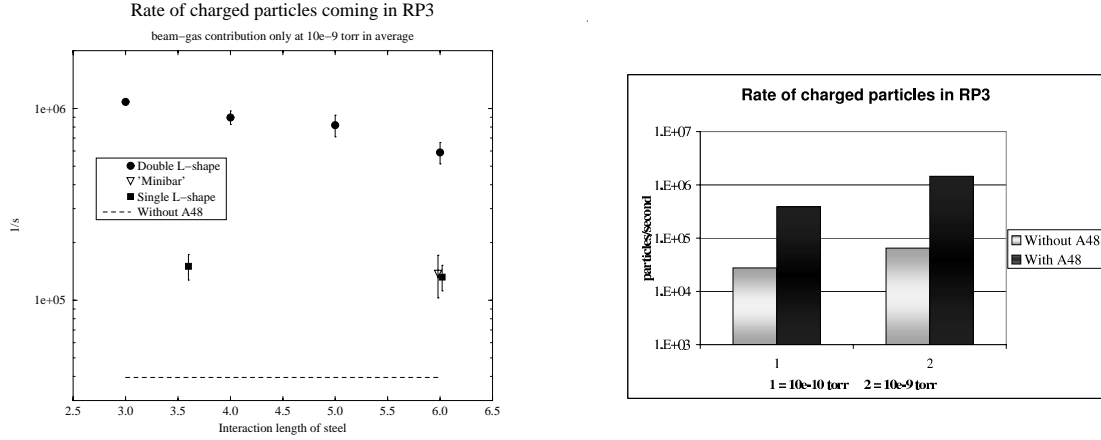


Figure 8: Rates of charged particles at RP3 as a function of the mask length for three shapes at 10^{-9} torr average pressure in Tevatron (left) and their sensitivity to the gas pressure (right). The dashed line corresponds to a case without the mask.

5 Abort Kicker Prefire

The STRUCT code was used to simulate proton beam loss at an AKP event [3]. Two configurations of A48 mask facing such a misbehaved beam have been considered in MARS simulations: a 1-m long “minibar” and 0.6-m long “single L-shape”. A spatial distribution of an AKP proton beam on the mask is shown in Fig. 9 (left). A corresponding charged particle fluence on the RP1 through RP3 pots is presented in Fig. 9 (right). From a practical standpoint, a 0.6-m mask is the preferable one. As shown in the previous section, a typical “operational” charged particle rate at the RP3 sensitive area is about $1.5 \times 10^5 \text{ s}^{-1}$. It corresponds to the yearly rate of 1.5×10^{12} integrated over a 10^7 second physics year. This is to be compared to the total number of charged particles at the same sensitive area for a single AKP contribution with the 0.6-m mask of 2.27×10^{12} . Therefore the nuisance for the RP generated by a single bunch hitting the collimator, even in the “minibar” version, is of the same order of magnitude as the beam-halo generated background accumulated over one year. The same is true for the CDF BHM (see Fig. 10).

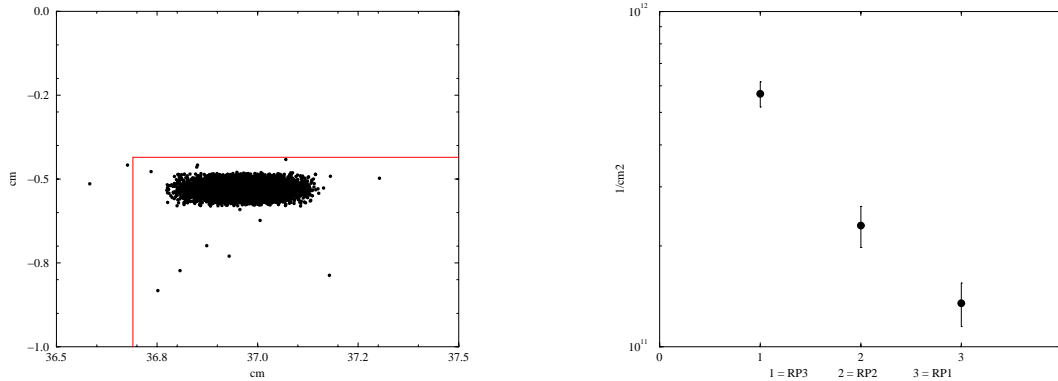


Figure 9: Spatial distribution of the AKP protons hitting a “minibar” A48 (left) and corresponding charged particle fluence at the RP1 – RP3 pots (right).

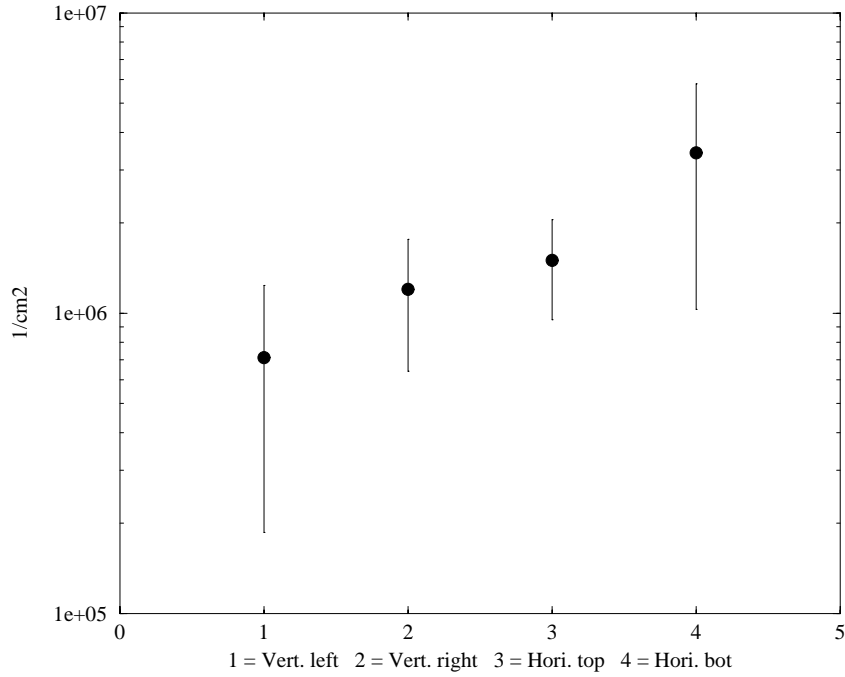


Figure 10: Charged particle flux in the CDF BHM due to AKP with the A48 protection.

6 DØ Roman pots

Although the DØ Roman Pots are of a different configuration than the CDF ones, one can get an idea of what they would undergo if another collimator would be placed upstream of DØ under similar conditions, in the event that the detector region needs to be protected against beam halo background. Fig. 11 compares the beam loss distributions upstream of the two detectors, considering the nuclear elastic beam-gas scattering only at average residual gas pressure in the ring of 10^{-9} torr. Ref. [1] predicts a loss rate upstream of DØ of 2.04×10^5 p/s to be compared to 1.87×10^5 p/s for CDF. A simple scaling allows one to obtain a prediction in the DØ case (Fig. 12 (left)). Here direct halo hits are not included and a contribution from secondaries only is shown. Direct hits would be a more important factor for the DØ RP, especially if they are placed closer to the beam than the CDF RP. The multiplication of secondaries due to a collimator would however follow the same behavior and be independent of the direct hits. The shielding efficiency of a shadow collimator for representative CDF (and DØ !) subdetectors is shown in Fig. 12 as a function of the distance from the IP for elastic beam-gas scattering as a source. One sees that such a mask reduces the backgrounds in the main detector by a factor of 4.5 to 25, at least for the elastic beam-gas component. This later was computed for CDF but is perfectly applied to DØ. The Beam Shower Counters (BSC) are about few centimeters to the beam pipe, whereas PLUG and BHM are at about one meter from the beam axis.

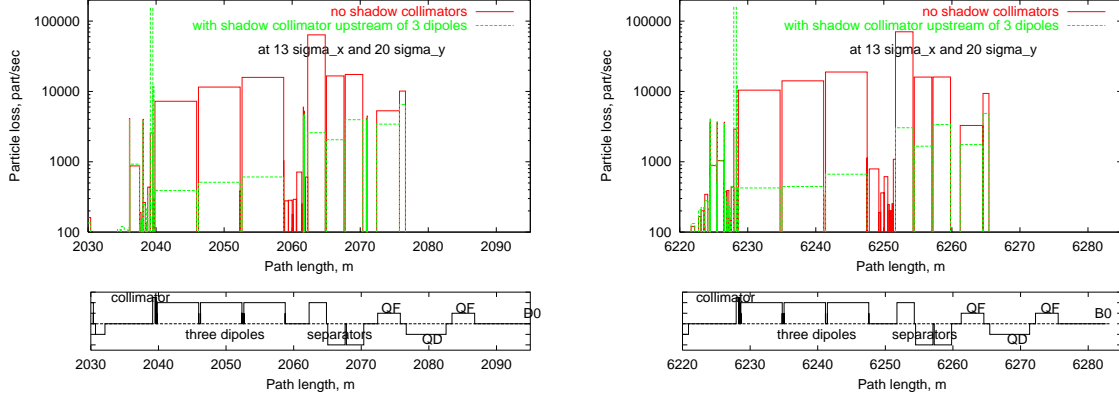


Figure 11: Beam loss distributions in the Tevatron interaction regions without shadow collimators and with a mask at $13\sigma_x$ and $20\sigma_y$ located upstream of the last three dipoles in front of the both IPs.

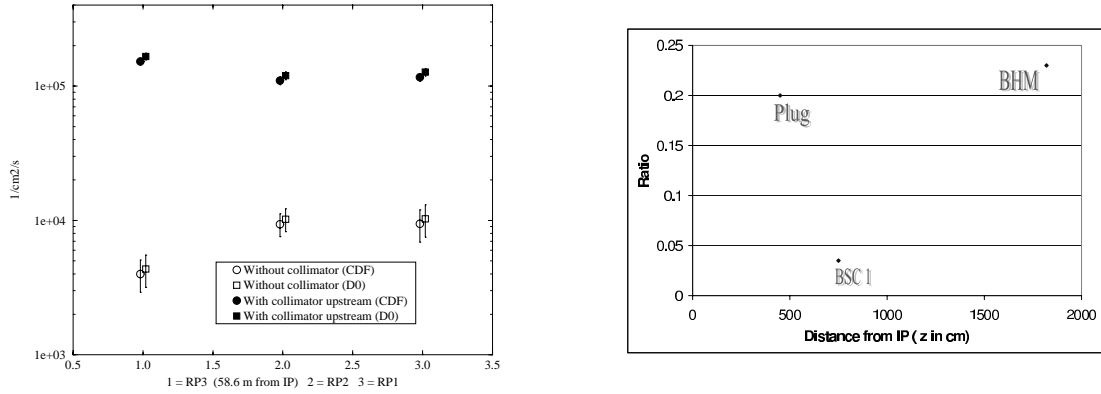


Figure 12: Charged particle flux at the DØ Roman Pots (left) and the main detector absorbed dose ratio with/without “double L-shaped” collimator for the elastic contribution as a function of the distance from the IP (right).

7 Conclusions

A MARS model of the CDF detector and BØ and DØ interaction regions has been created and benchmarked against experimental data, allowing to study the beam halo and AKP impact on the Fermilab collider detectors. The benchmark revealed that under the assumptions taken for these simulations, the average pressure of the Tevatron to be considered for future calculations seems to be around 10^{-10} torr. The model was used to investigate the implementation of the new collimator to be placed in front of the BØ and DØ IPs. It shows a very efficient protection for the main detectors against the beam-halo generated backgrounds in its “double L-shape” version, with somewhat reduced efficiency in the “minibar” version. It was shown that a “single L-shape” collimator would have the similar impact on the RP as the “minibar” at the same time keeping the option to offer more material to intercept beam halo since it is a mobile jaw, and that the length of the collimator is not a crucial aspect. In any event, the sensitive part of the RP should not be damaged by the radiation induced by the presence of the new collimator, but their background might reach 5 times its current value.

References

- [1] A.I. Drozhdin et al., “Backgrounds in the CDF and DØ Collider Detectors due to Nuclear Elastic Beam-Gas Scattering”, *to be published*.
- [2] <http://home.fnal.gov/nicolas/halo.html>.
- [3] A.I. Drozhdin, M.D. Church, “Tevatron Abort Kicker Prefire Simulations”, *to be published*.
- [4] <http://ncdf67.fnal.gov/~tesarek/radiation/>.
- [5] N.V. Mokhov, “The MARS Code System User’s Guide”, Fermilab-FN-628 (1995); N.V. Mokhov, O.E. Krivosheev, “MARS Code Status”, Proc. Monte Carlo 2000 Conf., p. 943, Lisbon, October 23-26, 2000; Fermilab-Conf-00/181 (2000); <http://www-ap.fnal.gov/MARS/>.
- [6] M.D. Church, A.I. Drozhdin, A. Legan, N.V. Mokhov, R.E. Reilly, “Tevatron Run-II Beam Collimation System”, *Proc. 1999 Particle Accelerator Conf.*, pp. 56-58, New York, March 29 - April 2, 1999; also Fermilab-Conf-99/059 (1999).
- [7] I.S. Baishev, A.I. Drozhdin, N.V. Mokhov, “STRUCT Program User’s Reference Manual”, SSCL-MAN-0034 (1994); <http://www-ap.fnal.gov/~drozhdin/>.